Double Phase Estimator: New Results

Daniele Borio

European Commission, Joint Research Centre (JRC),
Institute for the Protection and Security of the Citizen (IPSC),
Security Technology Assessment Unit,
Via Enrico Fermi 2749, 21027 Ispra (VA), Italy
Email: daniele.borio@ieee.org

***Abstract*—The Double Phase Estimator (DPE) has been recently proposed as an effective alternative to the Double Estimator (DE) for unambiguously tracking Binary Offset Carrier (BOC) modulated signals. In the DPE, the signal subcarrier is processed independently from the code and carrier components and it is tracked using a modified Phase Lock Loop (PLL). In the presence of signal bandlimiting, the DPE is able to generate local signal replicas better matched to the input components outperforming the DE.**

In this paper, the performance of the DPE are further characterized and, in particular, the concept of Subcarrier Multipath Error Envelope (SMEE) is introduced and used to analyse the multipath performance of DPE and DE. The analysis confirms the advantages of the DPE in the presence of signal bandlimiting.

***Index Terms*—Binary Offet Carrier, BOC, Double Estimator, Double Phase Estimator, DPE, GNSS, Signal Tracking**

I. Introduction

Modern Global Navigation Satellite Systems (GNSSs) adopt Binary Offset Carrier (BOC) modulations [1] to increase Radio Frequency (RF) compatibility among different signals and improve ranging accuracy. BOC modulations use an additional signal component, the subcarrier, to move the signal power away from the signal centre frequency and to obtain two main lobes displaced by f_{sub}, the subcarrier repetition frequency. The subcarrier significantly reduces interference issues and leads to signals with sharp autocorrelation functions, i.e. with improved ranging capabilities. BOC signals are however characterized by multi-peaked correlation functions and secondary peak lock can occur. Thus, several techniques have been designed to avoid secondary peak lock and to track unambiguously the main signal correlation peak. A review of the different unambiguous BOC tracking techniques can be found in [2], [3], [4]. These techniques can be divided in two groups: in the first one, the subcarrier is treated as a nuisance parameter which is either ignored or removed. In the second group, the subcarrier is recovered and fully exploited. Examples of techniques belonging to the second category are the Double Estimator (DE) [5], [6] and the Double Phase Estimator (DPE)[4] which can significantly outperform algorithms in the first group. In [4], it was concluded that
1) the subcarrier should be considered similarly to the signal code and carrier and not as a nuisance component causing ambiguity in the correlation function.
2) the subcarrier has characteristics intermediate between the code and carrier and thus it can be processed modifying techniques originally designed for these two signal components.

The first conclusion implies that a dedicated tracking loop, such as the Subcarrier Lock Loop (SLL) introduced by [5], [6], should be used for the the processing of the subcarrier component. Moreover, the subcarrier can be used for the generation of a new type of measurement: subcarrier phase observations. This is the approach commonly used for the processing of the code and of the carrier components which are tracked with a Delay Lock Loop (DLL) and a Phase Lock Loop (PLL), respectively. The output of these loops is then converted into code delay and carrier phase measurements.

The second conclusion implies that the subcarrier can be tracked either using a modified DLL, the SLL introduced by [6], or a modified PLL, the Subcarrier Phase Lock Loop (SPLL) introduced by [4]. The SPLL has a lower computation load than the SLL and has better performance, in terms of tracking jitter [7], in the presence of signal bandlimiting [4].

In this paper, the performance of the DPE is further studied. In particular the complex cross-correlation used by the SPLL to track the subcarrier is at first studied as a function of the input bandwidth of the receiver front-end. The DPE cross-correlation function is compared with that computed in the DE. From the analysis, it emerges that the DE outperforms the DPE only when the receiver front-end has a bandwidth sufficiently large to capture the main secondary lobes of the input BOC signal spectrum. This can be a stringent requirement on the receiver front-end.

The analysis performed on the correlation functions is then used as basis for characterizing the performance of the DPE and of the DE in the presence of multipath. The concept of Subcarrier Multipath Error Envelope (SMEE) is introduced and used to study the performance of the DPE and of the DE in the presence of multipath. The analysis shows that the two algorithms have similar performance in the presence of signal bandlimiting.

The remainder of the paper is organized as follows. Section II reviews the operating principles of the DPE and summarizes the results obtained in [4]. The cross-correlation functions obtained using the DPE are analysed in Section III and compared with that of the DE. The SMEE is analysed in Section IV and conclusions are finally drawn in Section V.

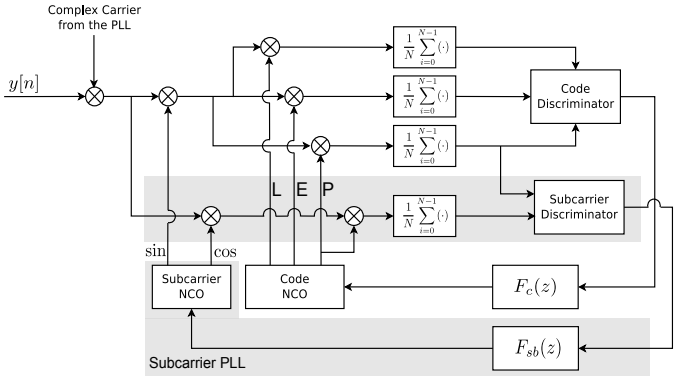

Fig. 1. Schematic representation of the DPE.

II. Double Phase Estimator

In this section, the operating principles of the DPE are briefly reviewed. In particular, a BOC modulated signal is made of four components:

$$x(t) = d(t)c(t)s_b(t)\cos\left(2\pi f_{RF}t\right) \tag{1}$$

where

- $d(t)$ is the navigation message containing the ephemerides and other navigation parameters
- $c(t)$ is a pseudo-random sequence selected from a family of quasi-orthogonal codes. $c(t)$ is Binary Phase Shift Keying (BPSK) modulated, i.e., each element of the code is represented as a constant (positive or negative) value
- $s_b(t)$ is the subcarrier obtained by periodically repeating a basic waveform
- the cosine term is the carrier which is used to up-convert the signal to the RF, f_{RF}.

The carrier and code components are usually processed using separated tracking loops, the PLL and the DLL, respectively. In traditional receiver architectures, the subcarrier is either processed jointly with the code or eliminated through non-linear operations. In [5], [6], an additional dedicated loop, the SLL, was introduced for the processing of the subcarrier component. In this case, the subcarrier was treated as the code component and processed using Early-minus-Late discriminators.

Eq. (1) models the transmitted signal and does not consider the effect of the receiver front-end on the subcarrier. This effect is considered by the DPE. In particular, [4] showed that the subcarrier of the received signal can be effectively approximated as a pure sinusoid in the presence of front-end filtering. For this reason, the SLL developed by [5] was replaced by a modified PLL, the SPLL, and the subcarrier was tracked similarly to the carrier component. A schematic representation of the DPE is provided in Fig. 1. The signal at the input of the DPE is denoted by $y[n]$. Note that $y[n]$ is a digital sequence obtained by sampling a filtered and down-converted version of the signal recovered by the receiver antenna. The residual signal Doppler effect is at first removed using the complex exponential generated by the PLL used to track the signal carrier component. Code and subcarrier components are then processed independently using a standard DLL and a SPLL, respectively. The SPLL uses an additional correlator, denoted as quadrature prompt correlator, to estimate the residual subcarrier phase error. This correlator is obtained by correlating the input signal with a local replica orthogonal to the input signal subcarrier. This orthogonal subcarrier is obtained by delaying of $T_{sub}/4$ the standard subcarrier used for the evaluation of the standard prompt correlator. $T_{sub} = \frac{1}{f_{sub}}$ is the subcarrier period.

In Fig. 1, the standard subcarrier is a sine wave, whereas the orthogonal subcarrier is a cosine wave. This choice is dictated by the fact that a *sine-phased* BOC modulation is considered in Fig. 1. When a *cosine-phased* modulation is considered, cosine and sine waves should be adopted for the generation of standard and quadrature components, respectively. Symbol N denotes the number of samples used for the signal correlation and $F_c(z)$ and $F_{sb}(z)$ are the transfer functions of the filters adopted by the DLL and the SPLL, respectively. In [4], the symbols P and P_Q are used to denote the standard and quadrature prompt correlators. Moreover, two SPLL discriminators were suggested:

$$\epsilon_c(\Delta\tau_s) = \frac{1}{2\pi f_{sub}}\arctan\left(\frac{\Re\{P_Q\}}{\Re\{P\}}\right) \tag{2}$$

$$\epsilon_{nc}(\Delta\tau_s) = \frac{1}{2\pi f_{sub}}\arctan\left(\Re\left\{\frac{P_Q}{P}\right\}\right). \tag{3}$$

Discriminator (2) is sensitive to residual phase errors from the PLL whereas (3) is non-coherent and can operate in the presence of residual phase errors. $\Delta\tau_s$ is the residual subcarrier delay error which leads to the discriminator outputs, ϵ_c and ϵ_{nc}, used to drive the SPLL.

In [4], the performance of the DPE was analysed in terms of coherent output Signal-to-Noise ratio (SNR), i.e. the SNR measured at the correlator output, and tracking jitter. It was shown that the DPE outperforms the DE in the presence of signal bandlimiting. Moreover, the DPE is more computationally efficient than the DE which requires the computation of an additional complex correlator.

In the next sections, the DPE is further analysed considering the correlation functions and the SMEE.

III. SPLL Correlation Function

In the DE and in the DPE techniques, a two-dimensional cross-correlation function is obtained [5]:

$$R_x(\tau_c,\tau_s) = \frac{1}{N}\sum_{n=0}^{N-1} y[n]c\left(nT_s-\tau_c\right)\bar{s}_b\left(nT_s-\tau_s\right) \tag{4}$$

where $y[n]$ is the digital sequence at the front-end output and $T_s = \frac{1}{f_s}$ is the sampling interval obtained as the inverse of the sampling frequency, f_s. Sequences $c(nT_s-\tau_c)$ and $\bar{s}_b\left(nT_s-\tau_s\right)$ are the code and subcarrier replicas locally generated by the receiver. Note that these two components are delayed independently by τ_c and τ_s, the code and subcarrier delays tested by the receiver. The symbol '-' has been introduced on the local subcarrier to indicate that a sequence

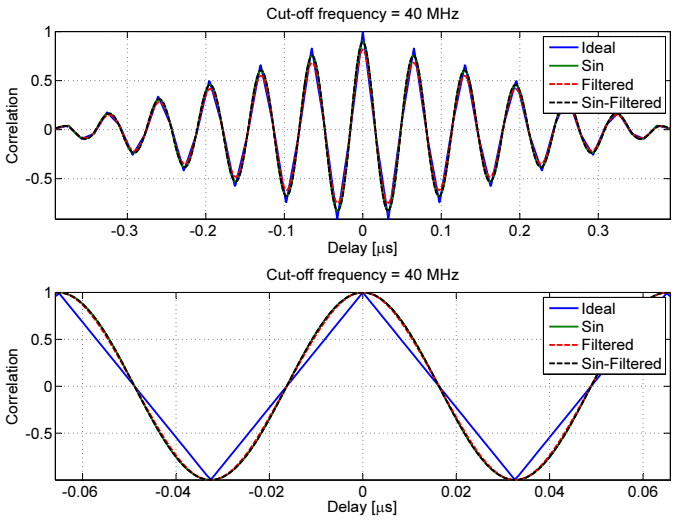

Fig. 2. Composite and subcarrier correlation functions of a cosine BOC(15, 2.5) signal in the presence of front-end filtering. Front-end cut-off frequency, $f_0 = 40$ MHz.

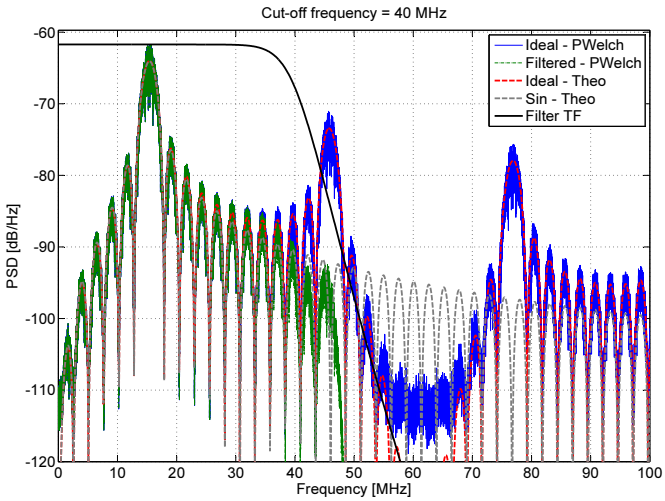

Fig. 3. PSDs of the different signal components used by the DE and PE. Front-end cut-off frequency, $f_0 = 40$ MHz, cosine BOC(15, 2.5) signal

different from the signal subcarrier, $s_b(\cdot)$, can be used for the computation of the cross-correlation, $R_x(\tau_c, \tau_s)$. The DE uses a subcarrier equal to that of the input signal, whereas the DE uses sinusoidal subcarriers. In (4), the impact of the residual carrier component is neglected.

From the two-dimensional cross-correlation, it is possible to extract

- the *code correlation*, when the subcarrier delay, τ_s, is matched to that of the incoming signal $y[n]$
- the *subcarrier correlation*, when the code delay, τ_c, is matched to that of the incoming signal $y[n]$
- the *composite correlation*, when the code and subcarrier delays are constrained to be equal, $\tau_c = \tau_s$. This is the correlation obtained by standard BOC tracking algorithms.

In the following, only the subcarrier and composite correlations are considered.

The front-end filter limits the frequency content of $y[n]$ introducing two main degradations: it rounds the main correlation peak and reduces its amplitude. The reduction of the correlation amplitude corresponds to the coherent output SNR loss investigated by [4]. The sensitivity of (4) to front-end filtering and signal bandlimiting mainly depends on the local subcarrier, $\bar{s}_b(\cdot)$. In the DPE, the local subcarrier is approximated by a pure sinusoid:

$$\bar{s}_b(t) = \sqrt{2}\sin(2\pi f_{sub} t) \tag{5}$$

where the case of sine-phased BOC modulations is considered. In this way, only the main frequency component of the input signal is retained during the evaluation of the cross-correlation function and thus the DPE is only marginally impacted by signal bandlimiting. This fact clearly emerges from Fig. 2 which shows the composite and subcarrier correlation functions for a cosine BOC(15, 2.5) signal in the presence of front-end filtering. Signal bandlimiting has been simulated by filtering the input signal with a Butterworth filter of order 9 and cut-off frequency, $f_0 = 40$ MHz. The curves denoted as 'Ideal' and 'Sin' are those obtained for the DE (square subcarrier wave) and for the DPE in the absence of filtering. No significant difference can be observed for the DPE: since only the first frequency component is retained, signal bandlimiting has almost no impact on the correlation process which implicitly performs filtering. This fact can be clearly seen from Fig. 3 which shows the Power Spectral Densities (PSDs) of the different signal components used by the DE and the DPE. The PSD of the DE local subcarrier is matched to the spectrum of the ideal signal, i.e., obtained in the absence of filtering. In this way, significant distortions can occur in the presence of signal bandlimiting. On the contrary, the sinusoidal subcarrier used by the DE recovers only the first main lobe of the signal PSD and, in this case, it is better matched to the spectrum of the input filtered signal. For this reason, the DE outperforms the DPE in the presence of signal bandlimiting.

In Fig. 2, both composite and subcarrier correlations are shown. The two correlations are provided in order to shown that, for small delays ($\tau_s < T_{sub}/2$), the two correlations assume similar values. The subcarrier correlations have been normalized in order to have the main peak equal to one. The normalization has been introduced to better analyse the impact of filtering on the sharpness of the correlation function. From the bottom part of Fig. 2, it emerges that when the front-end filter preserves only the main signal component, the DE and DPE operate on equivalent subcarrier correlation functions which can be effectively modelled as pure cosine waves. The composite correlation functions have not been normalized in order to better analyse the correlation amplitude reduction due to front-end filtering. A zoom of the main peak of the composite correlation functions is shown in Fig. 4: the filtered DE correlation function is the more impacted and suffers from the higher loss. This results is in agreement with the

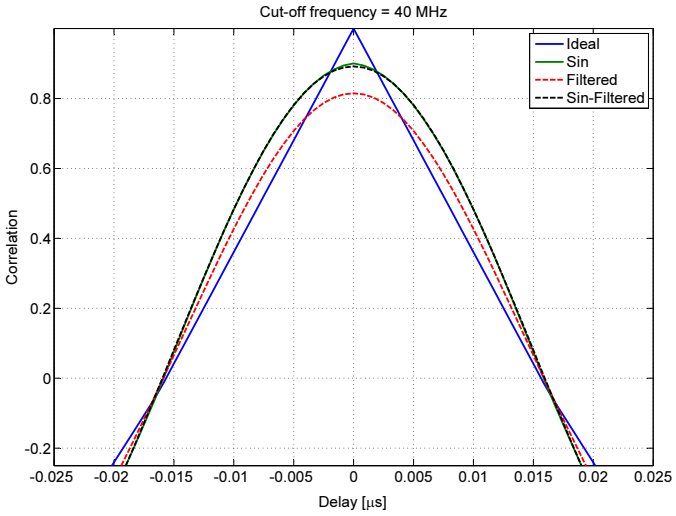

Fig. 4. Composite correlation functions of a cosine BOC(15, 2.5) signal in the presence of front-end filtering. Zoom of the main correlation peak. Front-end cut-off frequency, $f_0 = 40$ MHz.

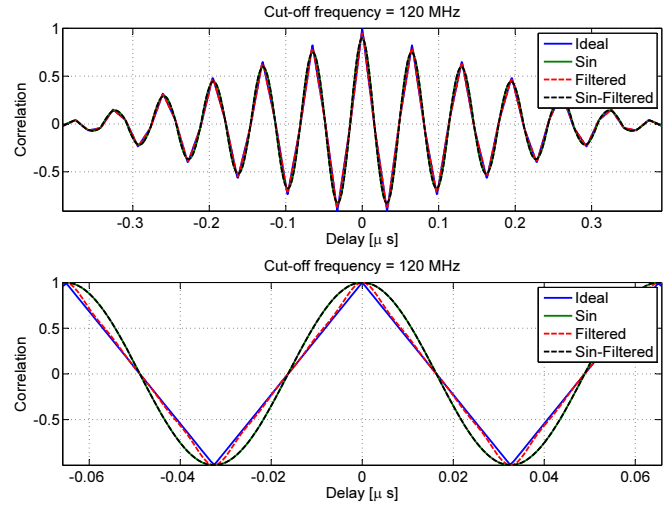

Fig. 5. Composite and subcarrier correlation functions of a cosine BOC(15, 2.5) signal in the presence of front-end filtering. Front-end cut-off frequency, $f_0 = 120$ MHz.

findings discussed in [4]. In particular, the DE outperforms the DPE only when the front-end filter has a bandwidth sufficiently large to acquire secondary main peaks of the BOC spectrum. For BOC modulated signals these peaks occur at the frequencies

$$f_{p,k} = (2k+1)f_{sub}, \qquad k = 0, 1, \ldots \quad . \tag{6}$$

Thus, for a cosine BOC(15, 2.5) signal (the modulation adopted by the Galileo E1a Public Regulated Service (PRS)), a front-end with a one-sided bandwidth larger than 45 MHz is required in order to fully exploit the benefits of the DE. This is a stringent requirement and the DPE should be preferred for receivers with narrower input filters. The composite and subcarrier correlation functions of a cosine BOC(15, 2.5) signal for a front-end cut-off frequency, $f_0 = 120$ MHz, are provided in Fig. 5. In this case, the advantages of the DE are clearly seen. Narrower correlation functions provide better multipath performance as discussed in Section IV.

IV. Subcarrier Multipath Error Envelope

The Multipath Error Envelope (MEE) is derived considering the one-path specular multipath model [8], [9]. In this case, the received signal is modelled as

$$r(t) = a_0 e^{j\phi_0} \left[x\left(t - \tau_0\right) + \alpha e^{j\phi_1} x\left(t - \tau_0 - \tau_1\right) \right] \tag{7}$$

where the impact of noise has been neglected and the signal Doppler frequency is assumed to be perfectly recovered by the receiver. The received signal, $r(t)$, is made of a Line-Of-Sight (LOS) component, with amplitude a_0 and phase ϕ_0, and a multipath component attenuated by α and rotated by an additional phase, ϕ_1. τ_0 is the delay of the LOS component and τ_1 is the excess multipath delay.
The receiver correlates signal (7) with local replicas of the code and subcarrier components and the following two-dimensional correlation is obtained:

$$\begin{aligned} \hat{R}(\tau_c, \tau_s) = a_0 e^{j(\phi_0 - \theta)} \left[R_x\left(\tau_c - \tau_0, \tau_s - \tau_0\right) \right. \\ \left. + \alpha e^{j\phi_1} R_x\left(\tau_c - \tau_0 - \tau_1, \tau_s - \tau_0 - \tau_1\right) \right] . \end{aligned} \tag{8}$$

where θ is the phase of the locally generated code and carrier components. As already mentioned in Section III, in the DE and the DPE a two dimensional correlation, $R_x(\tau_c, \tau_s)$, is obtained. In the literature [8], [9], [10], only a one-dimensional correlation function is considered. However, the multipath impact is generally evaluated separately on the code and carrier components. Also for the subcarrier the analysis should be conducted independently from the other signal components. For this reason, this paper considers the usage of a dedicated tracking loop for the processing of the subcarrier and extends the analysis determining the impact of multipath on the subcarrier delay.
For small residual delay errors, the two-dimensional function, $R_x(\cdot, \cdot)$, can be approximated as the product of the code and subcarrier correlations:

$$R_x(\tau_c, \tau_s) \approx R_c(\tau_c) \cdot R_s(\tau_s). \tag{9}$$

Moreover, it is possible to assume that the code correlation is approximatively constant for small delay errors. Thus, (8) can be rewritten only in terms of the subcarrier correlation function

$$\hat{R}(\tau_s) = a_0 e^{j(\phi_0 - \theta)} \left[R_s\left(\tau_s - \tau_0\right) + \alpha e^{j\phi_1} R_s\left(\tau_s - \tau_0 - \tau_1\right) \right] . \tag{10}$$

Correlation (10) can be used to evaluate the SMEE for the DPE and DE. The SMEE is defined similarly to the classical MEE for code and carrier measurements [10] and is area between the maximum and minimum error induced by a single multipath ray on the subcarrier observable. In the following, the SMEE is analysed for the DE and for the DPE.

A. DPE SMEE

In the DPE, the discriminator output is computed using (2) and (3) which require two correlation functions:

$$\begin{aligned} R_s(\tau_s) &= \cos(2\pi f_{sub}\tau_s) \\ R_s^o(\tau_s) &= R_s(\tau_s - T_{sub}/4) = \sin(2\pi f_{sub}\tau_s) \end{aligned} \tag{11}$$

where the first term corresponds to the standard prompt correlator and the second is related to the quadrature prompt correlator. Combining (11) with (10), the following composite correlations are found:

$$\begin{aligned} \hat{R}(\tau_s) &= a_0 e^{j(\phi_0-\theta)} \left[\cos\left(2\pi f_{sub}(\tau_s-\tau_0)\right)\right. \\ &\quad \left. +\alpha e^{j\phi_1}\cos\left(2\pi f_{sub}(\tau_s-\tau_0-\tau_1)\right)\right] \\ \hat{R}^o(\tau_s) &= a_0 e^{j(\phi_0-\theta)} \left[\sin\left(2\pi f_{sub}(\tau_s-\tau_0)\right)\right. \\ &\quad \left. +\alpha e^{j\phi_1}\sin\left(2\pi f_{sub}(\tau_s-\tau_0-\tau_1)\right)\right]. \end{aligned} \tag{12}$$

If the coherent discriminator is considered and under the assumption of small phase errors ($\phi_0 - \theta \approx 0$), only the real parts of (12) are used for the evaluation of the discriminator output. Moreover, (2) can be interpreted as the angle of

$$\Re\{P\} + j\Re\{P_Q\}$$

which corresponds to the complex correlation

$$\begin{aligned} &\Re\{\hat{R}(\tau_s)\} + j\Re\{\hat{R}^o(\tau_s)\} = a_0 e^{j2\pi f_{sub}(\tau_s-\tau_0)} \\ &\quad + \alpha\cos\phi_1 e^{j2\pi f_{sub}(\tau_s-\tau_0-\tau_1)} \\ &\quad = a_0 e^{j2\pi f_{sub}(\tau_s-\tau_0)}\left[1+\alpha\cos\phi_1 e^{-j2\pi f_{sub}\tau_1}\right]. \end{aligned} \tag{13}$$

Thus, the error on the subcarrier delay caused by the presence of a multipath ray is given by the phase of the second term of the last line of (13):

$$\tau_{ms} = \frac{1}{2\pi f_{sub}}\arctan\left(\frac{\alpha\cos\phi_1\sin(2\pi f_{sub}\tau_1)}{1+\alpha\cos\phi_1\cos(2\pi f_{sub}\tau_1)}\right). \tag{14}$$

The DE SMEE is finally obtained by maximizing and minimizing (14) with respect to the multipath excess phase, ϕ_1. In this way, the following expressions for the maximum and minimum multipath subcarrier errors are found:

$$\begin{aligned} \tau_{ms}^{max} &= \frac{1}{2\pi f_{sub}}\arctan\left(\frac{\alpha\left|\sin(2\pi f_{sub}\tau_1)\right|}{1+\alpha s\cos(2\pi f_{sub}\tau_1)}\right) \\ \tau_{ms}^{min} &= -\frac{1}{2\pi f_{sub}}\arctan\left(\frac{\alpha\left|\sin(2\pi f_{sub}\tau_1)\right|}{1-\alpha s\cos(2\pi f_{sub}\tau_1)}\right) \end{aligned} \tag{15}$$

where

$$s = \text{sign}\left[\sin(2\pi f_{sub}\tau_1)\right].$$

Eqs. (14)-(15) are similar to that reported in [10] for the code delay and show that the multipath delay error is always less then $\frac{1}{2\pi f_{sub}} \approx 0.16 T_{sub}$.

B. DE SMEE

In order to evaluate the SMEE for the DE, the numerical procedure depicted in Fig. 6 has been adopted. In particular, correlation (10) has been obtained by processing a signal affected by a multipath ray. Filtering has been accounted for by using a 9th order Butterworth filter. Filtered signals have been used to compute correlation (10) which, in turn, has been used to evaluate the S-curve defined by the SLL discriminator output. For the analysis detailed in the following, a normalized Early-minus-Late envelope discriminator has been considered:

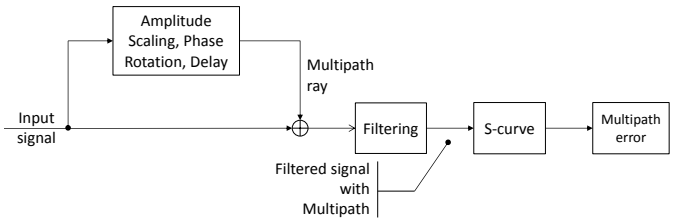

Fig. 6. Procedure for numerically evaluating the SMEE in the presence of filtering.

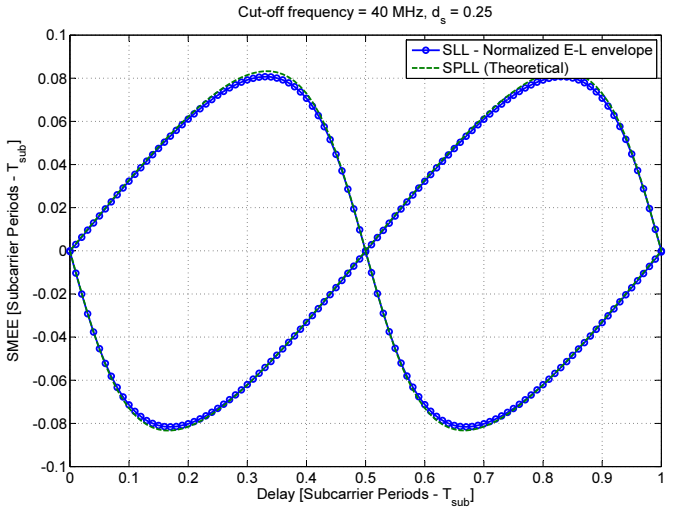

Fig. 7. SMEE evaluated in the presence of front-end filtering for the DE and DPE. $\alpha = 0.5$.

$$S(\tau_s) = \frac{|E_s(\tau_s)| - |L_s(\tau_s)|}{|E_s(\tau_s)| + |L_s(\tau_s)|} \tag{16}$$

where $|E_s(\tau_s)|$ and $|L_s(\tau_s)|$ are the subcarrier Early and Late correlators [5] obtained by correlating the input signal with local subcarriers delayed by $\pm d_s/2$, respectively. d_s is the subcarrier Early-minus-Late spacing. The performance of the DE depends on d_s. The presence of a multipath signal biases the S-curve which is equal to zero for $\tau_s \neq 0$. The delay that makes $S(\tau_s) = 0$ is the multipath error. An iterative procedure has been used to find this delay and evaluate the multipath error for fixed values of α and τ_1. The multipath error has been evaluated as a function of ϕ_1 and an exhaustive search has been adopted to find the minimum and maximum delay errors which define the SMEE.

C. Results

The approaches described above have been used for evaluating the SMEE for the DE and the DPE. The SMEEs evaluated in the presence of front-end filtering are provided in Fig. 7. The SMEE has been evaluated for a cosine BOC(15, 2.5) signal in the presence of signal bandlimiting with a cut-off frequency $f_0 = 40$ MHz. The results have been expressed in terms of

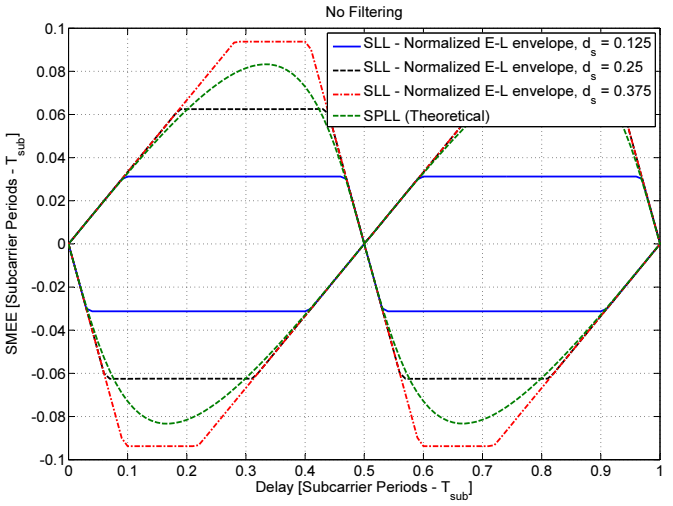

Fig. 8. SMEE evaluated in the absence of front-end filtering. The subcarrier spacing used by the DE impacts the SMEE.

the subcarrier period that, in this case, is equal to $65,17$ ns and corresponds to approximatively 20 metres. The SMEE is periodic with period, $T_{sub}/2$. This fact is expected since the S-curves from which it is derived are also periodic with period, $T_{sub/2}$. In this case, $\alpha = 0.5$ and the multipath error is always less then $0.083T_{sub}$ which corresponds to approximately 1.66 metres. An Early-minus-Late spacing $d_s = 0.25T_{sub}$ has been considered for the DE. The two techniques have similar SMEEs showing similar performance. This is due to the fact that, in the presence of filtering, the correlation function processed by the DE can also be approximated by a pure sinusoid which, in turn, leads to an approximately sinusoidal S-curve. This curve is affected by multipath in a similar way as the DPE. Early-minus-Late subcarrier spacings in the range $[0.0625 - 0.375]T_{sub}$ have been tested and it has been verified that, in the presence of filtering, d_s has a limited impact on the multipath performance of the DE: front-end filtering does not allow the full exploitation of the benefits of the narrow correlator approach [7].

The SMEE analysis has been repeated in Fig. 8 in the absence of front-end filtering. In this case, the benefits of narrow chip spacings and the advantages of the DE with respect to the DPE clearly appear. The DPE is outperformed by the DE in the absence of front-end filtering. These results show that the DPE and the DE have similar performance in terms of SMEE when only the first main lobe of the BOC spectrum is retained by the receiver front-end.

V. Conclusions

In this paper, the performance of the DPE, a recently proposed unambiguous BOC tracking technique, has been analyzed and compared with that of the DE. In the DPE, the subcarrier is treated independently from the code and carrier components and is used for the generation of subcarrier delay measurements. Moreover, the subcarrier is considered similarly to the carrier component and is tracked using a modified PLL.

The analysis has been conducted in terms of correlation function and MEE accounting for the impact of front-end filtering. In particular, the concept of SMEE has been introduced and a closed-form expression for the SMEE of the DPE has been derived. From the analysis, it emerges that the DPE and DE have similar multipath performance in the presence of front-end filtering. The DE outperforms the DPE only if the receiver front-end is able to recover the secondary main lobes of the BOC spectrum. This could be a stringent requirement for the processing wideband signals such as the cosine BOC(15, 2.5) adopted by the Galileo E1a PRS signal and the DPE should be preferred for receivers with narrow input filters. This slight performance degradation is however compensated by the lower computational load of the DPE.

References

[1] J. W. Betz, "Binary offset carrier modulations for radionavigation," *NAVIGATION, the Journal of the Institute of Navigation*, vol. 48, no. 4, pp. 227–246, Winter 2001.

[2] P. Anantharamu, "Space-time equalization techniques for new GNSS signals," PhD Thesis, Schulisch School of Engineering, University of Calgary, Sep. 2011.

[3] J. Wendel and S. Hager, "A robust technique for unambiguous BOC tracking," in *Proc. of the 26th International Technical Meeting of the Satellite Division of The Institute of Navigation (ION GNSS+)*, Nashville, TN, Sep. 2013, pp. 1–12.

[4] D. Borio, "Double phase estimator: a new unambiguous binary offset carrier tracking algorithm," *IET Radar, Sonar & Navigation*, vol. 8, no. 7, pp. 729–741, Aug. 2014.

[5] M. S. Hodgart, P. Blunt, and M. Unwin, "The optimal dual estimate solution for robust tracking of binary offset carrier (BOC) modulation," in *Proc. of the 20th International Technical Meeting of the Satellite Division of The Institute of Navigation (ION GNSS)*, Fort Worth, TX, Sep. 2007, pp. 1017–1027.

[6] M. Hodgart and P. Blunt, "Dual estimate receiver of binary offset carrier modulated signals for global navigation satellite systems," *Electronics Letters*, vol. 43, no. 16, pp. 877 –878, 2 2007.

[7] A. J. Van Dierendonck, P. Fenton, and T. Ford, "Theory and performance of narrow correlator spacing in a GPS receiver," *NAVIGATION: Journal of the Institute of Navigation*, vol. 39, no. 3, pp. 265 –283, Fall 1992.

[8] A. Van Dierendonck, "Ch. 5, GPS receivers," in *Global Positioning System Theory and Applications*, B. W. Parkinson and J. J. Spilker Jr., Eds. American Institute of Aeronautics & Astronautics, 1996, vol. 1, pp. 329–407.

[9] M. S. Braasch, "On the characterization of multipath errors in satellite-based precision approach and landing systems," PhD Thesis, College of Engineering and Technology, Ohio University, Jun. 1992.

[10] M. Smyrnaios, S. Schön, and M. L. Nicolás, "Multipath propagation, characterization and modeling in GNSS," in *Geodetic Sciences - Observations, Modeling and Applications*. InTech, May 2013, ch. 2, pp. 99–126.